Fractionating Nanosilver: Importance for Determining Toxicity to Aquatic Test Organisms

ARTICLE *in* ENVIRONMENTAL SCIENCE & TECHNOLOGY · NOVEMBER 2010

Impact Factor: 5.33 · DOI: 10.1021/es1025382 · Source: PubMed

Environ. Sci. Technol. **2010,** *44,* 9571–9577

Fractionating Nanosilver: Importance for Determining Toxicity to Aquatic Test Organisms

ALAN J. KENNEDY,*,† MATTHEW S. HULL,‡ ANTHONY J. BEDNAR,† JENNIFER D. GOSS,† JONAS C. GUNTER,§ JENNIFER L. BOULDIN,|| PETER J. VIKESLAND,‡ AND JEFFERY A. STEEVENS†

U.S. Army Engineer Research and Development Center, Vicksburg, Mississippi 39180, United States, Department of Civil and Environmental Engineering, Virginia Polytechnic Institute and State University, Blacksburg, Virginia, United States, Luna Innovations, Blacksburg, Virginia, United States, and Arkansas State University, Jonesboro, Arkansas, United States

Received July 26, 2010. Revised manuscript received October 18, 2010. Accepted October 21, 2010.

This investigation applied novel techniques for characterizing and fractionating nanosilver particles and aggregates and relating these measurements to toxicological endpoints. The acute toxicity of eight nanosilver suspensions of varying primary particle sizes (10−80 nm) and coatings (citrate, polyvinylpyrrolidone, EDTA, proprietary) was assessed using three aquatic test organisms (*Daphnia magna*, *Pimephales promelas, Pseudokirchneriella subcapitata*). When 48-h lethal median concentrations (LC50) were expressed as total silver, both *D. magna* and *P. promelas* were significantly more sensitive to ionic silver (Ag^+) as $AgNO_3$ (mean LC50 = 1.2 and 6.3 μg/L, respectively) relative to a wide range in LC50 values determined for the nanosilver suspensions (2 −126 μg/L). However, when LC50 values for nanosilver suspensions were expressed as fractionated nanosilver (Ag^+ and/or <4 nm particles), determined by ultracentrifugation of particles and confirmed field-flow-fractograms, the LC50 values (0.3−5.6 μg/L) were comparable to the values obtained for ionic Ag^+ as $AgNO_3$. These results suggest that dissolved Ag^+ plays a critical role in acute toxicity and underscores the importance of characterizing dissolved fractions in nanometal suspensions.

Introduction

Environmental health and safety (EHS) researchers are tasked with determining fate and effects of diverse nanoparticles that likely represent extremes in environmental behavior and toxicological implications (e.g., carbon versus metal based materials). Separating nanomaterials into chemical classes or similarly behaving categories may be the first step for simplifying risk characterization (*1*). A recent joint workshop hosted by the Engineer Research and Development Center and the National Institute of Standards and Technology (7−8 April 2009, Vicksburg, MS, USA) addressed only nanosilver (nAg) to focus EHS research and answer basic and applied questions. The incorporation of nAg into a growing list of applications including antimicrobial coatings for medical devices, home appliances, water treatment, inks, and fabrics (*2*) has raised concern provided the potential release of Ag from those products (*3, 4*) in concert with the known toxicity of ionic Ag^+ to fish and invertebrates (*5*−*8*). According to the Project on Emerging Nanotechnologies, nAg is referenced in more commercial products than other nanomaterials combined (http://www.nanotechproject.org/inventories/consumer/analysis_draft/; accessed April 20, 2010), although this survey may not be inclusive of products failing to disclose nanomaterial ingredients. An additional complication for EHS work is scaling down the large number of nAg materials and synthesis methods; for instance, nAg particles can be manufactured by top-down or bottom up processes, at different sizes, and with different reactants and capping agents (*2*).

One question is whether nAg is a new introduction of an old legacy contaminant (i.e., traditional Ag) (*9*) or if special consideration to particulate size or other unique attributes is needed; however, traditional Ag contamination in the environment is suspected to be predominately colloidal associations relative to the ionic phase (*5*). A great deal of study has addressed the toxicity of Ag releases due to previous industrial practices (e.g., photographic film industry) (*5*). The Ag ion (Ag^+) is the second most toxic metal after mercury (*6*) to freshwater fish and invertebrates (*6*−*8, 10*). The mechanism of Ag^+ toxicity is impairment of sodium−potassium active transport that reduces the ability of freshwater organisms to ionoregulate within hypotonic solution leading to cardiovascular collapse (*7*). This toxicity, however, is mitigated in the environment by metastable sulfide, chloride and organic matter complexes (*5, 7*). Previous research has reported that nAg suspensions have the potential to induce toxicity to biological receptors at much lower levels (low μg/L *11*−*13*) relative to some purified carbon nanomaterials (*14, 15*) that require high concentrations (mg/L) unlikely to be observed in the environment. Blaser et al. (*4*) theoretically determined that concentrations of nAg in the environment may reach 15% of all Ag measured, although current water concentrations are generally relatively low (<0.46 μg/L (*5*)).

The objectives of this study were to assess the toxicity of a variety of manufactured nAg materials in suspension, compare nAg toxicity to the toxicity of ionic Ag^+, and to relate toxicity to the particulate and ionic fractions in the nAg suspensions. Toxicity was assessed using a freshwater fish larva (*Pimephales promelas*) and a zooplankton species (*Daphnia magna*). Lethal median concentration (LC50) values were expressed in terms of both total measurable Ag and fractionated nAg (defined below). An algae species (*Pseudokirchneriella subcapitata*) was also tested for comparison. Although consideration of Ag^+ complexation and bioavailability is important, the intent of this study was solely to compare the toxicity of various nAg suspensions in laboratory test systems.

Experimental Section

Test Materials. A review by Tolaymat et al. (*2*) reported that the majority of nAg in the literature is circum-spherical, synthesized by bottom-up processing using silver nitrate ($AgNO_3$) and generally stabilized using citrate or polyvi-

* Corresponding author phone: (601)634-3344; fax: (601)634-2263; e-mail: Alan.J.Kennedy@usace.army.mil. Corresponding author address: U.S. Army Engineer Research and Development Center, Environmental Laboratory, EP-R, 3909 Halls Ferry Rd, Vicksburg, MS 39180.

† U.S. Army Engineer Research and Development Center.

‡ Virginia Polytechnic Institute and State University.

§ Luna Innovations.

|| Arkansas State University.

10.1021/es1025382
Published on Web 11/17/2010

nylpyrrolidone (PVP). We selected such nAg materials of different manufacturers and coatings to potentially relate particle characteristics to toxicity. Nanosilver particle dispersions with the nominal sizes of 10, 20, 50, and 80 nm (NC10, NC20, NC50, and NC80) were obtained from NanoComposix (Biopure, San Diego, CA, USA). PVP coated nAg (PVP-nAg) was fabricated at Luna Innovations (Blacksburg, VA, USA) by addition of 75 mL of ethylene glycol to a round-bottom flask in a heating mantle. PVP (1.5 g, molecular weight = 10,000) was allowed to dissolve with magnetic stirring and 0.050 g of $AgNO_3$ was added before heating and stirring in a sealed flask (1 °C/min to 120 °C, maintained for 1-h). The mixture was immersed in a room temperature water bath and dialyzed against deionized water (10,000 MWCO dialysis tubing) to reduce ethylene glycol, unbound PVP, and Ag^+. Citrate and EDTA (ethylenediaminetetraacetic acid) stabilized nAg (EDTA-nAg) were fabricated at Virginia Tech (Blacksburg, VA, USA). Citrate coated nAg (citrate-nAg) was produced by citrate reduction of $AgNO_3$. Briefly, a 1 mM solution of $AgNO_3$ and a 10 mM solution of trisodium citrate were added to a 200 mL round-bottom flask (2:1 v/v) and boiled in a water bath (40−50 min). For EDTA-nAg, 1 mL of 26 mM $AgNO_3$ was added to a mixture containing 100 mL of 0.16 mM EDTA and 4 mL of 0.1 M NaOH under vigorous stirring. Finally, a commercially sold colloidal silver drink (ASAP, American Biotech Laboratories, Alpine, UT, USA) labeled as 10 mg/L (verified as 10.3 mg/L by ICP-MS) was tested as a currently used product relevant for environmental release. A reagent grade $AgNO_3$ salt (CAS No. 7761-88-8, Sigma Aldrich, Catalog No. 204-390-50G, St. Louis, MO, USA) was also tested to determine test organism sensitivity to ionic silver (Ag^+).

Acute Toxicity of Nanosilver Suspensions. Acute toxicity tests were conducted due to the known rapid onset of Ag^+ toxicity to fish and invertebrates. The animal species tested were the freshwater cladoceran *Daphnia magna* (<24-h old, in-house cultures, originally from Aquatic Biosystems, Fort Collins, CO, USA) and the fathead minnow *Pimephales promelas* (1-d old, Aquatic Biosystems). Bioassays were conducted at 25 ± 2 °C in basic accordance with guidance (*16, 17*), and mortality was assessed in five quadruplicated and analytically confirmed exposure concentrations. Moderately hard reconstituted water (MHRW), formulated to a hardness of 80 mg/L as $CaCO_3$ (U.S. EPA 2002), was used as control and dilution water. To determine the impact of nAg on a lower trophic group, the alga *Pseudokirchneriella subcapitata* (formerly *Selenastrum capricornutum)* was exposed to PVP-nAg, as this material represented the nAg suspension with the lowest fraction of dissolved Ag. Algae were cultured and tested at Arkansas State University Ecotoxicology Research Facility, according to guidance (*17*). Working suspensions of PVP nAg were prepared in Bold's Basal media without EDTA. Algal growth inhibition tests were performed in a Conviron Growth Chamber (Model 8507; Controlled Environments Limited, Winnipeg, Manitoba, Canada) on an orbital shaker. Constant rotation was maintained at 100 cpm with continuous illumination at 4300 ± 430 lx. Cell counts on a hemacytometer were used to obtain 96-h endpoints.

Characterization and Analytical Chemistry. Size was determined for both dry particles and for suspended particle aggregates. Subsets of particle suspensions (10−20 μL) were imaged using Transmission Electron Microscopy (Zeiss 10CA, 60 kV, Oberkochen, Germany), and the longest dimension was analyzed for all particles (>70 particles exception: ASAP-nAg = 30 since few particles were found) using Image J software (U.S. National Institutes of Health). The hydrodynamic diameter of particles in aqueous suspension was determined by two methods after mixing 10 mg/L stocks 1:1 with either Milli-Q (MQ) water (Milli-Q Plus ultrapure water system, Millipore, 18.2 mΩ/cm, Billerica, MA, USA) or a 580 μS/cm water (the 1:1 dilution of the stock in MQ water resulted in 290 μS/cm moderately hard reconstituted water, or MHRW) and allowing either 0 or 24-h equilibration. The first method was dynamic light scattering, or DLS (90 Plus/BI-MAS, Brookhaven Instruments, Holtsville, NY, USA), with data expressed as intensity of light scattered. The second method was Field Flow Fractionation interfaced to Inductively Coupled Plasma Mass Spectrometry (FFF-ICP-MS), using a PostNova (Salt Lake City, UT, USA) F-1000 symmetrical flow FFF and a Perkin-Elmer (Waltham, MA) Elan DRC-II ICP-MS. Separation of nominal 20, 50, and 100 nm polystyrene bead size standards (PostNova) was obtained using a channel flow of 1 mL/min and a cross-flow of 0.75 mL/min in a mobile phase of 0.025% FL-70 surfactant (Fisher Scientific, Fair Lawn, NJ) + 0.025% sodium azide (Sigma-Aldrich, St. Louis, MO). The membrane used was made from regenerated cellulose (1 kDa). An Agilent (Santa Clara, CA) 1100 HPLC UV absorbance detector was used to monitor elution of the polystyrene bead standards and to construct a calibration curve of size versus retention time. The ICP-MS plasma was operated at 1250W and interfaced to the FFF with a MiraMist nebulizer (argon flow rate of 0.8 L/min) and Scott spray chamber. Both ^{107}Ag and ^{109}Ag isotopes were monitored, each with a 500 ms dwell time such that one data point was collected approximately each second. The number of readings per replicate (1800) was selected such that a continuous Ag fractogram was collected for approximately 30 min. Under these separation conditions, the 20 nm size standard was baseline resolved from the injection void peak. Additional FFF-ICP-MS methodology is available in the literature (*18*). Electrophoretic mobility (and indirectly zeta potential) were determined as previously described (*15*).

Fractionation of Nanosilver. The nAg suspensions were fractionated by three methods. An initial attempt using low molecular weight cutoff filter centrifuge tubes (Millipore, Amicon Ultra-4-Ultracel UFC800596 and UFC810096, Tullagreen, Carrigtwohill, County Cork, Ireland) to separate dissolved from particulate Ag was unacceptable as 5 and 100 kDa membranes removed 57% and 48% of Ag^+ as $AgNO_3$, respectively, from a 4 mL aliquot of 33.5 mg Ag^+/L solution. The second method, hereafter referred as fractionated nAg, involved ultracentrifugation of 8 mL samples at 100,000 × g for 60 min (Beckman Optima XL-80K ultracentrifuge, Rotor 70.1 Ti, Brea, CA, USA), a force calculated to move particles (>4 nm diameter) at least 2.5 cm. Thus, 1.5 mL supernatant was sampled from the top of the centrifuge tubes and acidified with nitric acid (Thermo Fisher Scientific, CAS No. 7697-37-2, Catalog No. A200-212, Fairlawn, NJ, USA). Similar techniques were previously employed (*11*). Preliminary experiments using concentrated stocks (20−100 mg Ag/L) resulted in an obvious pellet at the bottom of the centrifuge tube. This procedure was applied to both nAg stocks and for the test media. The third method utilized FFF separation in which the relative fraction of dissolved Ag in the nAg suspensions was determined by integrating the fractogram void peak and the particle peak, as determined using the polystyrene bead standards. Samples were diluted using 3% nitric acid (v/v) prior to analysis in all experimental solutions was analyzed by ICP-MS using a PerkinElmer Elan DRC-II. As with the FFF analyses, both Ag isotopes were monitored, with the more abundant ^{107}Ag used for quantitation and the ^{109}Ag isotope used for confirmation. In all analyses, ^{103}Rh was added online using a mixing "T" as an internal standard to correct for instrumental drift. Reporting limits for silver ranged from 0.5 to 1.0 μg/L.

Statistical Analysis. The normality and homogeneity of data distributions were determined by Shapiro-Wilks and Bartlett's Tests, respectively. Lethal median concentrations (LC50) and effective concentrations (EC50), including 95% confidence intervals ($CI_{95\%}$), were determined using ToxCalc

version 5.0 (Tidepool Scientific Software, McKinleyville, CA, USA) applying the trimmed Spearman-Karber method. Statistical significance between LC50 values was defined as nonoverlapping $CI_{95\%}$. Pearson Product Moment and Spearman Rank Order correlation analysis were conducted using SigmaStat Software (SPSS, Chicago, IL, USA).

Results and Discussion

Our results indicate that the tested nanosilver (nAg) suspensions were significantly less acutely toxic than the disassociated Ag^+ ion as $AgNO_3$. The two nAg fractionation methods discussed (ultracentrifugation and FFF) corroborated one another and provided evidence that the fractionated nAg in the tested nAg suspensions was more predictive of acute toxicity than total measurable Ag. We caveat that, if present, it is possible that smaller particles (<4 nm) may be included in this fraction.

Characterization. The nAg particles were circum-spherical, with the exception of some 23 by 150 nm rods in the citrate-nAg and smaller rods in the NC20 and NC50 samples (Figure 1; Table 1); NC20 and 50 may have included some smaller than nominal particles (Figure 1e,f). The primary particle size reported by the manufacturer and determined from our TEM images (Figure 1) was consistently smaller than that determined by DLS and FFF (Table 1). This was expected as hydrodynamic diameter by definition increases in aqueous media (*19*), particles aggregate in suspension, and the intensity of light scattered in polydisperse suspensions is skewed toward larger particles (*19*). The trend was especially notable for the PVP-nAg and NC10. Comparison of values in Table 1 and Pearson correlation indicated particle sizing by FFF (Figure S1) ($r = 0.64$; $p = 0.13$) was better related to primary particle size by TEM relative to DLS ($r = 0.09$; $p = 0.86$), although agreement between FFF and DLS hydrodynamic size was reasonably good for some materials (citrate-nAg, EDTA-nAg, NC20, NC50, NC80) or approximated the smaller DLS size range (EDTA-nAg, NC10, PVP-nAg). Pearson correlations were stronger for the primary particle size (by TEM) of NanoComposix materials (NC10, NC20, NC50 and NC80) related to DLS ($r = 0.80$; $p = 0.41$) and FFF ($r = 0.91$; $p = 0.09$); for these materials, DLS and FFF were strongly related ($r = 0.99$; $p = 0.08$). Further, there was general agreement between TEM, FFF, and DLS measurements of suspensions with large particle size distributions (citrate-nAg, NC20, NC50). For DLS, an acceptable autocorrelation was attained for all suspensions, with the baseline index exceeding 6.0 (exception: NC10 in MQ water, EDTA-Ag in MHRW; Supporting Information, Table S1) and particle kilocounts per second (kcps) ranging from 300−500 (exception: NC10 in MQ water = 23 kcps, NC80 in MQ water = 1000 kcps). Agreement was found between particle size by FFF with the smaller particle size populations from the DLS measurements (e.g., NC10, 9−28 nm, Table 1). This suggests that larger particle aggregates reported by DLS were retained in the FFF past the analytical runtime (30 min fractogram corresponding to approximately 110 nm) or eliminated from the FFF analysis by the addition of surfactant. The zeta potential (Table 1) of particle suspensions ranged from −15 to −46 mV. Electrophoretic mobility is provided in the Supporting Information (Table S2).

Only 24-h after spiking, the increased ionic strength (conductivity = 290 μS/cm) of MHRW significantly increased hydrodynamic diameters (DLS, FFF) relative to that in ultrapure water (0 μS/cm) (Table 1). Some materials (NC10, NC20, NC50, EDTA-Ag) appeared yellow in suspension at 5 mg/L but turned orange, blue, and then gray after a few hours in the higher ionic strength medium. The PVP-Ag (red) and NC80 (gray) suspensions did not change in color after 24-h. The polydispersity of particles in MHRW either remained similar to MQ water or decreased slightly. However,

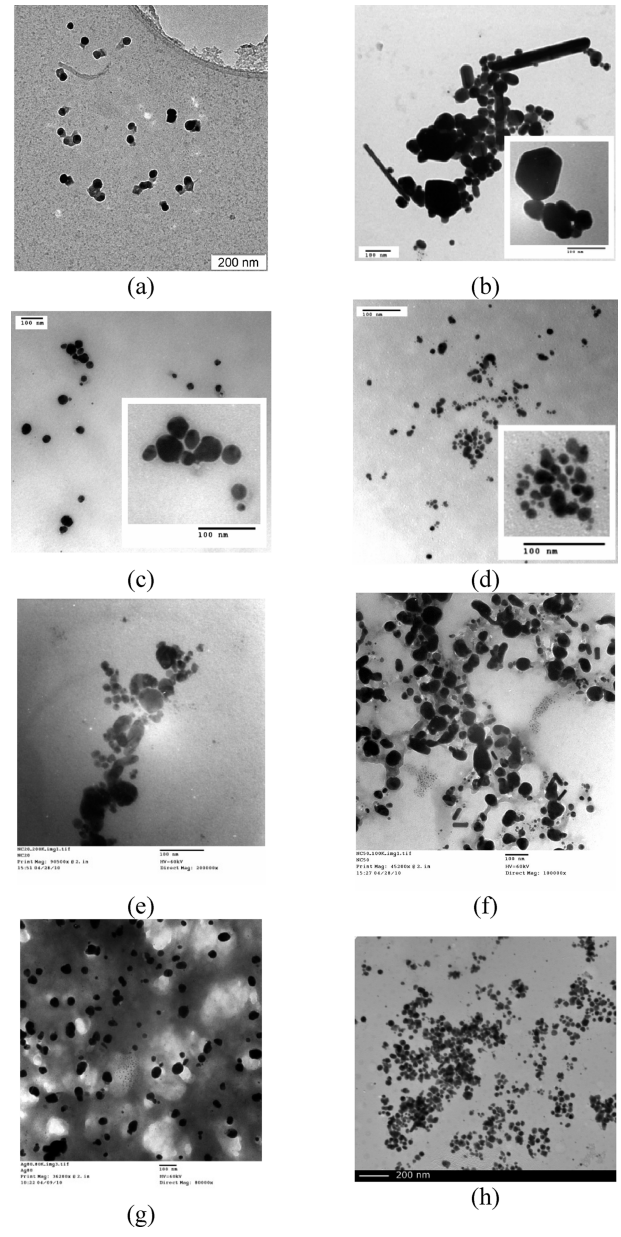

FIGURE 1. Images of test materials by scanning: (a) ASAP-Ag, and transmission electron microscopy: (b) citrate-nAg, (c) EDTA-nAg, (d) NanoComposix 10, (e) NanoComposix 20, (f) NanoComposix 50, (g) NanoComposix 80, and (h) PVP-nanosilver.

the rate of aggregation is affected by both the collapse of the diffuse double layer of counterions around the particle and the frequency of particle-to-particle interactions, a side effect of concentration (*19*). Therefore, nAg suspensions at lower concentrations (i.e., toxicologically relevant range of 1 to 100 μg/L) may be less aggregated than in the higher concentration samples required for DLS, FFF, and zeta potential measurements, and it is therefore possible that the nAg particles used in the bioassays were less aggregated than suggested (Table 1). Unfortunately, as noted by Domingos et al. (*19*), most analytical equipment is unable to accurately characterize nAg suspensions at toxicologically relevant concentrations ($\ll$1 mg/L).

Fractionation of Nanosilver. Stocks, pellets, and supernatants of PVP-nAg, citrate-nAg, and EDTA-nAg in deionized water were analyzed to assess the suitability of ultracentrifugation for separating suspensions into dissolved and particulate fractions and to determine suspension charac-

TABLE 1. Nano-Silver (nAg) Materials Tested[f]

material	TEM (nm)	FFF (nm)[a]	hydrodynamic diameter by intensity (nm) MQ water	hydrodynamic diameter by intensity (nm) MHRW	zeta potential[b] (mV)
ASAP-nAg	31 (63%)	*c*	185 ± 5 (67−80; 200−263)	228 ± 4 (171−310)	NA
Citrate-nAg	29 (57%)[d]	61 (31−90)	70 ± 1 (26−43; 71−137)	77 ± 1 (26−43; 90−167)	−46 ± 3
EDTA-nAg	36 (35%)	29 (10−52)	59 ± 0 (18−26; 84−120)	204 ± 4 (55−75; 268−400)	−33 ± 1
NanoComposix (10 nm)	10 (53%)	19 (10−31)	85 ± 4 (9−28; 116−374)	310 ± 4 (121−153; 388−520)	−21 ± 2
NanoComposix (20 nm)	20 (80%)	27 (14−40)	27 ± 0 (13−71)	ND	−23 ± 1
NanoComposix (50 nm)	49[e] (46%)	58 (40−81)	55 ± 0 (11−21; 48−93)	ND	−34 ± 1
NanoComposix (80 nm)	50 (35%)	92 (69−111)	101 ± 1 (36−45; 112−163)	117 ± 1 (61−111; 160−290)	−20 ± 1
polyvinyl pyrrolidone Ag	41 (31%)	35 (19−73)	96 ± 0 (14−32; 55−271)	96 ± 1 (14−32; 55−272)	−15 ± 1

[a] Approximate peak width provided in parentheses. [b] Approximated from Smoluchowski's model, with electrophoretic mobility reported in the Supporting Information. [c] ASAP-Ag did not form a stable suspension under the FFF separation conditions precluding size determination. [d] Rods with a mean width of 23 ± 8 nm and mean length of 150 ± 47 nm were also found (Figure 1b). [e] Less than 5 nm particles observed but not included in analysis (see Figure 1e). Median size is 12 nm (CV = 96%) when small particles included. [f] Size of particles from transmission electron microscopy (TEM) is expressed as the median value (coefficient of variation in parentheses). Aqueous size was determined by field flow fractionation (FFF). Additionally, mean hydrodynamic diameter (size ranges in parentheses) in Milli-Q (MQ) and moderately hard reconstituted water (MHRW) were determined by dynamic light scattering (DLS) after 24-h equilibration. Zeta potential is reported in MQ water and other test media (Supporting Information, Table S2).

TABLE 2. 48-h Lethal Median Concentration (LC50) Values for (a) *Daphnia magna* and (b) *Pimephales promelas*[a]

material	toxicity rank (as total Ag)	total Ag	fractionated Ag
	(a)		
		0.7 (0.1−0.8)	NA
$AgNO_3$	1	1.3 (1.2−1.5)	NA
		1.6 (1.3−1.8)	NA
ASAP	2	1.8 (1.6−2.0)	0.3 (0.3−0.4)
NanoComposix 10	3	5.4 (3.5−7.0)*	0.6 (0.5−0.6)
NanoComposix 20	3	5.3 (4.9−5.7)*	ND
NanoComposix 50	3	5.4 (4.4−6.5)*	ND
Citrate-nAg	4	11.1 (10.2−14.1)*	1.2 (1.0−1.6)
EDTA-nAg	5	14.9 (12.4−18.0)*	0.9 (0.9−1.0)
NanoComposix 80	6	17.7 (15.8−19.8)*	ND
PVP-nAg	7	97.0 (87.2−107.9)*	1.9 (1.7−2.2)
	(b)		
		5.7 (5.2−6.2)	NA
$AgNO_3$	1	6.5 (6.2−6.9)	NA
		6.6 (6.2−7.0)	NA
ASAP	2	9.0 (8.1−10.0)*	1.5 (1.3−1.7)#
Citrate-nAg	3	19.2 (16.8−21.9)*	4.1 (3.5−6.1)
NanoComposix 10	4	41.0 (34.5−48.8)*	4.3 (3.7−5.0)#
EDTA-nAg	5	55.2 (47.4−65.9)*	1.5 (1.4−1.5)#
NanoComposix 50	6	60.7 (52.2−70.6)*	3.5 (2.8−4.5)#
NanoComposix 20	7	64.1 (56.5−72.8)*	4.5 (3.3−5.7)
NanoComposix 80	8	125.6 (112.6−140.1)*	5.6 (4.5−7.6)
PVP-nAg	NA	>69.9 *	NA

[a] Values (μg/L) are expressed as total and measurable silver after centrifugation (i.e., fractionated Ag). Significantly greater (asterisks) and lower (number signs) values relative to $AgNO_3$ are based on 95% confidence limits. NA = not available; ND = not detected (< 0.5 μg/L).

teristics. The PVP-nAg stock concentration was 90 mg Ag/L, and the mean mass of triplicate pellet and supernatant samples was 211 ± 16 μg Ag and 2.0 ± 1.3 μg Ag, respectively. A mass balance elucidated 91% mass recovery in the pellet and supernatant, with 97% and 3% in the pellet and supernatant, respectively. The method was also applied to a citrate-nAg stock (5.55 mg/L) with 101% recovery and 7.3 ± 1.0 μg settled particle (71%) and 1.1 ± 0.2 μg in the supernatant (29%). The ultracentrifugation and FFF methods (Figure S1) for fractionating particulate from "dissolved" Ag were within 2% between the methods (Table S3, Supporting Information), with the exception of heterogeneous citrate-nAg (14% difference) which could be the result of the nonspherical particles observed by TEM. Dissolved fractions of the tested nAg suspensions ranged from 2 to 57%, although most suspensions were in the range of 2−8% (Table S3, Supporting Information). Previous studies involving toxicological testing of nAg have reported dissolved percentages of 0.7−1.2% (*12*), 0.45 to 3.7% (*13*), 7% (*26*), and negligible (*11*).

Acute Toxicity of Nanosilver Suspensions. Mean (ranges in parentheses) water quality parameters for bioassays were acceptable; temperature = 24.2 (23.0−25.1) °C, conductivity = 303 (270− 390) μS/cm, pH = 8.06 (7.44−8.76), dissolved oxygen >5.9 mg/L). The LC50 values acquired for ionic Ag^+ as $AgNO_3$ (Table 2) were within range of reported 48-h values of 0.6−2.9 μg/L for *D. magna* (*8, 20*) and 48 to 96-h values of 6.7−14.0 μg/L for *P. promelas* (*8, 21, 22*) exposed in similar water conditions. *Daphnia magna* was significantly more sensitive to Ag^+ than *P. promelas* (Table 2) and the alga *P. subcapitata* (96-h EC50 = 9.9 [7.4−13.2] μg/L); it is generally

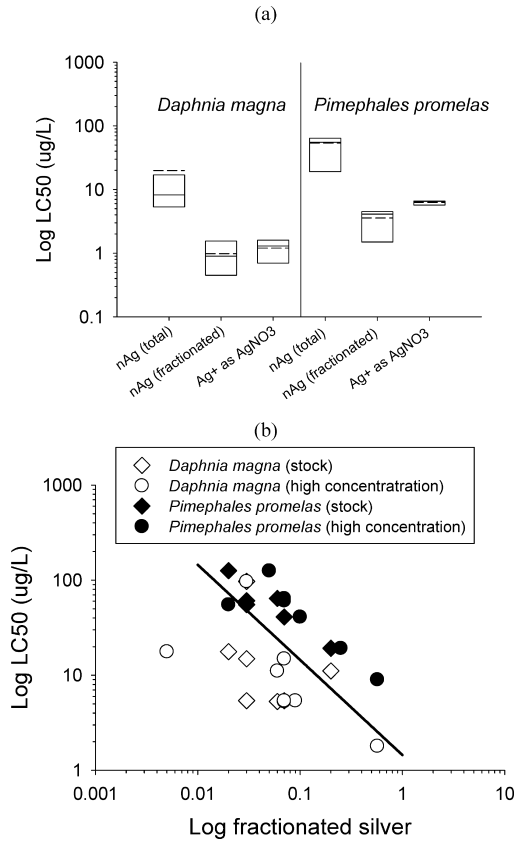

FIGURE 2. Lethal median concentrations (LC50) related to fractionated nanosilver (nAg). Panel (a) provides box plots of the LC50 distributions as ionic Ag^+ ($AgNO_3$), total and fractionated silver (Ag). The 75% data percentile (boxes), median (solid lines), and mean (dashed lines) are indicated. Note that the PVP-nanosilver LC50 value for *D. magna* was significantly higher than the other materials (Table 2), explaining positioning of the arithmetic mean. Panel (b) illustrates an inverse relationship between LC50 values and fractionated nAg (by ultracentrifugation). For comparative purposes, the line represents an inverse third order polynomial model of the 48-h LC50 for $AgNO_3$ divided by the ionic fractions (Ag^+) of theoretical nAg suspensions ($y = -6.5254 \times 10^{-16} + (1.45/x) + (-1.1414 \times 10^{-17}/x^2) + (8.4421 \times 10^{-20}/x^3)$).

supported that cladocerans are more sensitive to Ag^+ than fish or algae (*5*).

Ionic Ag^+ as $AgNO_3$ was more acutely toxic (48-h) than total measurable Ag (which included suspended nAg) for all three test species, with most mortality occurring within 24 h. Relatively higher ionic Ag^+ toxicity compared to nAg is supported in the literature for different test species (*11, 12, 23*). The toxicity of the nAg suspensions tested in this study were strongly dose-dependent (Supporting Information, Figure S2) and ranged from 1.4−75, 1.4−19, and 2 times less toxic (depending on the material) than Ag^+ to *D. magna, P. promelas*, and *P. subcapitata*, respectively (Figure 2a). These ranges bracket previous reporting that nAg was 4 to 5 times less toxic than ionic Ag^+ (*11*). However, relatively lower loss of nAg in suspension (as total Ag) occurred during the 48-h exposures in the present study (6−37%; exception NC10: 52%) compared to the previous (>90%) study (*11*). While the algae was less sensitive to Ag^+ than animal receptors, as reported in this study and by Griffitt et al. (*11*), it was more sensitive to PVP-nAg (EC50 = 18.4 [10.6−31.9]; 21 [14.6−30.2] μg/L; compare to Table 2). The enhanced algae sensitivity to PVP-nAg may relate to the surfactant properties of ethylene glycol, which may not be completely removed by dialysis, as surfactants are employed to disrupt membranes during algae blooms (*24*). Overall for the different nAg suspensions, a large range in acute lethality values (Table 2) was observed for *D. magna* (1.8 to 97 μg/L) and *P. promelas* (9.0−125.6 μg/L), as reported for other fish and cladocerans (9.4 to 67 μg/L; 11,13). The large ranges in the above LC50 values imply that total measurable Ag is not an appropriate predictor of nAg toxicity, and future studies need to report additional information, such as the dissolved fraction of Ag (Figure 2b).

Fractionated nAg (our definition of dissolved) concentrations in the nAg suspensions were more predictive of acute toxicity. When the LC50 values generated for the nAg suspensions in the present study were expressed as fractionated nAg, the LC50 values for *D. magna* decreased significantly (0.3 to 1.9 μg/L), becoming comparable to $AgNO_3$ toxicity (Table 2; Figure 2a). For *P. promelas*, fractionated nAg LC50 (1.5−5.6 μg/L) values were also more comparable, albeit slightly lower, to those for $AgNO_3$ relative to LC50 values expressed as total Ag (Table 2). The most toxic material (expressed as total measurable Ag), ASAP-nAg, had the highest "dissolved" fraction (57%), while the least toxic material, PVP-nAg, had the lowest "dissolved" fraction (3%) (Table S3). While in the present study the fractionated nAg appeared to explain much of the acute lethality, Griffitt et al. (*11*) reported that Ag^+ did not explain all toxicity observed for nAg exposure to *D. pulex* and *Ceriodaphnia dubia* and later published toxicogenomics information suggesting that zebrafish exposed to nAg and Ag^+ had distinct gene expression profiles (*25*). Genomic changes due to nAg have not yet been related to observable effects on fish (*25, 26*) and may be more relatable to chronic effects. Laban et al. (*13*) reported that dissolved Ag^+ in nAg exposures was less toxic than $AgNO_3$ to *P. promelas*, although testing was at a much higher hardness (240 mg/L relative to 80 mg/L) and the authors suggested that the slow release of Ag^+ from the nAg may have facilitated complexation. Further, ionic Ag^+ may sorb to nAg particles (*27*), implying high particle concentrations will provide more surfaces for Ag^+ to bind. Navarro et al. (*12*), however, supported the conclusion that ionic Ag^+ determined toxicity; while EC50 values for algae were not solely explained by the dissolved concentration of nAg, they concluded that additional nAg dissolved during the exposure dictated the discrepancy. Finally, robust historical testing of Ag contamination in environmental water has demonstrated that while Ag exists as complexes in the colloidal form (<0.45 μm), geochemical species analysis suggests toxicity to trout is best demonstrated by dissolved Ag^+ (*5, 7*). Data generated from this study and previous work suggest that while the available ionic Ag^+ fraction in the nAg suspensions is much more toxic than nAg itself, determining the cause of chronic toxicity of nanosilver particles may be more complex.

The LC50 values for *D. magna* exposed to all nAg suspensions expressed as fractionated Ag were within the 95% confidence intervals of the LC50 for ionic Ag^+ as $AgNO_3$ (Table 2). It is not known why the LC50 values expressed as fractionated nAg^+ for some suspensions (EDTA-Ag, NC10, ASAP-Ag; Table 2) did not match $AgNO_3$ toxicity for *P. promelas* as closely as observed for *D. magna*. It is possible that nAg dictates a larger role in determining toxicity at anatomical features unique to the fish (particle binding and dissolution at the gills *25, 28*) or an increase in the relative fraction of dissolved Ag occurred during the fish exposure, as suggested for algae exposed to nAg (*12*), causing the calculated LC50 value to be lower. We observed a slight but consistent increase in dissolved Ag^+ at the NOECs of the *P. promelas* exposures (Table S4, Supporting Information), although we caveat that this increase was small (0.5−2.7 μg/L) and close to detection limits. Clearly further study is needed to definitively determine if different species interactions with nAg dispersions may influence dissolution kinetics.

The NanoComposix materials (NC10, NC20, NC50, NC80) were inversely related to the LC50 values for *P. promelas* by Pearson Product Moment correlation relative to nominal particle size ($r = 0.90$; $p = 0.10$; $n = 4$) and FFF hydrodynamic diameter ($r = 0.91$; $p = 0.09$; $n = 4$), indicating a trend of decreasing toxicity with increasing particle size (Table 2). No significant fit was found for DLS effective diameter ($p = 0.52$) due to an unexpectedly high effective diameter for NC10 (Table 1). An impurity or precipitant was observed in our preparation of the NC10 stock, which may have confounded the DLS result to a relatively higher effective diameter. The fit excluding the NC10 data, albeit not significant, improves ($r = 0.91$; $p = 0.27$; $n = 3$). However, the narrow range in LC50 values for these four nAg suspensions expressed as fractionated nAg (3.5−5.6 μg/L) still suggests that fractionated Ag was a reasonable predictor of toxicity for the tested suspensions (Figure 2; Table 2), with the nominal particle size ($r = -0.97$; $p = 0.03$; $n = 4$) and hydrodynamic diameter by FFF ($r = -0.97$; $p = 0.04$; $n = 4$) being inversely Pearson correlated to fractionated nAg in the highest exposure concentration. For *D. magna*, no significant difference in the toxicities of NC10, NC20, and NC50 was found, although significantly lower toxicity was observed for the largest particle suspension (NC80).

Since a two parameter hyperbolic decay ($R = 0.71$, $p < 0.01$) was observed between the fractionated nAg and toxicity (Figure 2b), Spearman correlations of ranks were used to compare the 48-h LC50 values for each of the nAg materials. There was a strong correlation ($r = 0.90$; $p = 0.08$) between *D. magna* and *P. promelas* LC50 values (measured as total Ag) that were significantly different (NC20, NC50 excluded for *D. magna*), suggesting correspondence in interspecies sensitivity to the tested nAg suspensions. Correlation between LC50 values and primary particle size by TEM indicated trends for *D. magna* ($r = 0.77$; $p = 0.10$) and *P. promelas* ($r = 0.57$; $p = 0.15$). There was no correlation between LC50 and FFF estimated size or aggregate size by DLS. No significant fit was found between dissolved Ag^+ by FFF-ICP-MS for *D. magna* or *P. promelas* LC50 values ($p > 0.45$), which may be related to the nature of the integration under the FFF fractogram being an estimation that does not provide resolution in the range of 2 to 7%. However, data generated from the ultracentrifugation fractionation method resulted in a reasonable fit for LC50 values and fractionated nAg in the stock (*D. magna*: $r = -0.80$, $p = 0.13$; *P. promelas*: $r = -0.94$; $p = 0.02$) and a significant fit to fractionated nAg in the highest test concentrations (*D. magna*: $r = -0.79$, $p = 0.03$; *P. promelas*: $r = -0.78$; $p = 0.03$).

The findings from this study and previous work (*11, 12, 25*) emphasize a need for researchers to measure the particle and dissolved (or smaller particle) fraction of Ag over the duration of toxicological bioassays to understand the nature of the exposure. Further, when the research objectives are to determine only the toxicity associated with the nanoparticle itself, it is important to minimize the presence of ions and residual reactants (e.g., reducing agents). Purification of nAg suspensions may be necessary to remove dissolved Ag that can occur due to incomplete reduction of silver salts (e.g., $AgNO_3$) during nanoparticle synthesis (*2*) or the tendency of nAg particles to settle (*11*) or dissolve during exposures, though such steps may only reset dissolved Ag^+ concentrations and promote additional particle dissolution. The potential for dissolved Ag^+ to exist in excess in nAg suspensions will also be contingent on the test media, organism physiology and processing (*25*), dissolution kinetics and equilibrium and whether coatings may passivate dissolution. These considerations need to be made in context with ligands (e.g., organic matter) in natural waters. Research is necessary to derive a standardized method for measuring the particulate and dissolved fractions of nanometals. Further, studies investigating dissolution kinetics are needed, including consideration to organism loading after the dissolution of nanometal has come into equilibrium with the test medium (*5*). Studies are needed to determine if very small particles (<4 nm) present in the concentrated stocks of larger nanoparticles may dissolve once diluted into higher ionic strength exposure media. Unfortunately current characterization methods for nanoparticles are not capable of assessing particle size and aggregate state at toxicologically relevant concentrations (low μg/L), and most environmental fate research is conducted at much higher concentrations (mg/L).

Acknowledgments

We thank James Ranville, Colorado School of Mines for SEM images of ASAP-Ag. This research was conducted under the Environmental Quality Technology Program of the US Army ERDC (Dr. John Cullinane). Permission was granted by the Chief of Engineers to publish this information. The authors also thank Drs. David Johnson and Karl Indest (ERDC) and four anonymous reviewers for their thoughtful comments.

Supporting Information Available

Additional supportive data are provided for DLS quality control measures (Table S1), zeta potential and electrophoretic mobility (Table S2), total and dissolved silver in nanosilver stocks (Table S3), changes in total and dissolved silver concentrations during bioassays (Table S4), field flow fractograms of the nanosilver suspensions (Figure S1), and plot of test animal dose dependency and nanosilver (Figure S2). This material is available free of charge via the Internet at http://pubs.acs.org.

Literature Cited

(1) Tervonen, T.; Linkov, I.; Figueira, J. R.; Steevens, J.; Chappell, M.; Merad, M. Risk-based classification system of nanomaterials. *J. Nanopart. Res.* **2009**, *11*, 757–766.

(2) Tolaymat, T. M.; El Badawy, A. M.; Genaidy, A.; Scheckel, K. G.; Luxton, T. P.; Suidan, M. An evidence-based perspective of manufactured silver nanoparticle in synthesis and applications: A systematic review and critical appraisal of peer-reviewed scientific papers. *Sci. Total Environ.* **2010**, *408*, 999–1006.

(3) Benn, T. M.; Westerhoff, P. Nanoparticle silver released into water from commercially available sock fabrics. *Environ. Sci. Technol.* **2008**, *42*, 4133–4139.

(4) Blaser, S. A.; Scheringer, M.; MacLeod, M.; Hungerbuhler, K. Estimation of cumulative aquatic exposure and risk due to silver: contribution of nano-functionalized plastics and textiles. *Sci. Total Environ.* **2008**, *390*, 396–409.

(5) *Silver in the environmental: transport, fate and effects*; Andren, A. W., Bober, T. W., Eds.; Society of Environmental Toxicology and Chemistry: Pensacola, FL, 2002.

(6) Ratte, H. T. Bioaccumulation and toxicity of silver compounds: a review. *Environ. Toxicol. Chem.* **1999**, *18*, 89–108.

(7) Hogstrand, C.; Wood, C. M. Toward a better understanding of the bioavailability, physiology, and toxicity of silver in fish: implications for water quality criteria. *Environ. Toxicol. Chem.* **1998**, *17*, 547–561.

(8) Erickson, R. J.; Brooke, L. T.; Kahl, M. D.; Venter, F. V.; Harting, S. L.; Markee, T. P.; Spehar, R. L. Effects of laboratory test conditions on the toxicity of silver to aquatic organisms. *Environ. Toxicol. Chem.* **1998**, *17*, 572–578.

(9) Luoma, S. N. Silver nanotechnologies and the environment: Old problems or new challenges. Project on Emerging Nanotechnologies is supportedby the Pew Charitable Trusts, 2008, PEN 15. http://www.pewtrusts.org/our_work_report_detail.aspx?id=44004 (accessed July 20, 2010).

(10) Ferguson, E. A.; Hogstrand, C. Acute silver toxicity to seawater-acclimated rainbow trout: influence of salinity on toxicity and silver speciation. *Environ. Toxicol. Chem.* **1998**, *17*, 589–593.

(11) Griffitt, R. J.; Luo, J.; Gao, J.; Bonzongo, J. C.; Barber, D. S. Effects of particle composition and species on toxicity of metallic nanomaterials in aquatic organisms. *Environ. Toxicol. Chem.*, **2008**, *27*, 1972–1978.

(12) Navarro, E.; Piccapietra, F.; Wagner, B.; Marconi, F.; Kaegi, R.; Odzak, N.; Sigg, L.; Behra, R. Toxicity of silver nanoparticles to

Chlamydomonas reinhardtii. *Environ. Sci. Technol.* **2008**, *42*, 8959–8964.
(13) Laban, G.; Nies, L. F.; Turco, R. F.; Bickham, J. W.; Sepulveda, M. S. The effects of silver nanoparticles on fathead minnow (*Pimephales promelas*) embryos. *Ecotoxicol.* **2010**, *19*, 185–195.
(14) Zhu, S.; Oberdorster, E.; Haasch, M. L. Toxicity of an engineered nanoparticle (fullerene, C60) in two aquatic species, *Daphnia* and fathead minnow. *Mar. Environ. Res.* **2006**, *62*, S5–S9.
(15) Kennedy, A. J.; Gunter, J. C.; Chappell, M. A.; Goss, J. D.; Hull, M. S.; Kirgan, R. A.; Steevens, J. A. Influence of nanotube preparation in aquatic bioassays. *Environ. Toxicol. Chem.* **2009**, *28*, 1930–1938.
(16) *Methods for Measuring the Acute Toxicity of Effluents and Receiving Waters to Freshwater and Marine Organisms*; EPA/812/R/02/012; U.S. Environmental Protection Agency, Office of Water: Washington, DC, 2002.
(17) *Short Term Methods for Estimating the Chronic Toxicity of Effluents and Receiving Water to Freshwater Organisms*, 4th ed.; EPA/812/R/02/013; U.S. Environmental Protection Agency, Office of Water: Washington, DC, 2002.
(18) Dubascoux, S.; El Hecho, I.; Hassellov, M.; Von Der Kammer, F.; Potin Gautier, M.; Lespes, G. Field-flow fractionation and inductively coupled plasma mass spectrometer coupling: History, development, and applications. *J. Anal. At. Spectom.* **2010**, *25*, 613–23.
(19) Domingos, R. F.; Baalousha, M. A.; Ju-nam, Y.; Reid, M. M.; Tufenkji, N.; Lead, J. R.; Leppard, G. G.; Wilkinson, K. J. Characterizing manufactured nanoparticles in the environment: multimethod determination of particle sizes. *Environ. Sci. Technol.* **2009**, *43*, 7277–7284.
(20) *Comprehensive report: Interlaboratory comparison: acute testing set*; EPA-600/3-81-005; Lemke, A. E., U.S. Environmental Protection Agency: Duluth, MN, 1981.
(21) Lima, A. R.; Curtis, C.; Hammermeister, D. E.; Call, D. J.; Felhaber, T. A. Acute toxicity of silver to selected fish and invertebrates. *Bull. Environ. Contam. Toxicol.* **1982**, *29*, 184–189.
(22) Holcomb, G. W.; Phipps, G. L.; Fiandt, J. T. Toxicity of selected priority pollutants to various aquatic organisms. *Ecotoxicol. Environ. Saf.* **1983**, *7*, 400–409.
(23) Bianchini, A.; Grosell, M.; Gregory, S. M.; Wood, C. M. Acute silver toxicity in aquatic animals is a function of sodium uptake rate. *Environ. Sci. Technol.* **2002**, *36*, 1763–1766.
(24) Kennedy, A. J.; Millward, R. N.; Steevens, J. A.; Lynn, J. W.; Perry, K. D. Relative sensitivity of zebra mussel (*Dreissena polymorpha*) life-stages to two copper sources. *J. Great Lakes Res.* **2006**, *32*, 596–606.
(25) Griffitt, R. J.; Hyndman, K.; Denslow, N. D.; Barber, D. S. Comparison of molecular and histological changes in zebrafish gills exposed to metallic nanoparticles. *Toxicol. Sci.* **2009**, *107*, 404–415.
(26) Scown, T. M.; Santos, E. M.; Johnston, B. D.; Gaiser, B.; Baalousha, M.; Mitov, S.; Lead, J. R.; Stone, V.; Fernandes, T. F.; Jepson, M.; van Aerle, R.; Tyler, C. R. Effects of aqueous exposure to silver nanoparticles of different sizes in rainbow trout. *Toxicol. Sci.* 2010. *in press*.
(27) Liu, J.; Hurt, R. H. Ion release kinetics and particle persistence in aqueous nano-silver colloids. *Environ. Sci. Technol.* **2010**, *44*, 2169–2175.
(28) Griffitt, R. J.; Weil, R.; Hyndman, K. A.; Denslow, N. D.; Powers, K.; Taylor, D.; Barber, D. S. Exposure to copper nanoparticles causes gill injury and acute lethality to zebrafish (*Danio rerio*). *Environ. Sci. Technol.* **2007**, *41*, 8178–8186.

ES1025382